Backgrounds at the Next Linear Collider *

S.S. Hertzbach
University of Massacheusetts, Amherst MA 01003
T.W. Markiewicz, T. Maruyama, R. Messner
Stanford Linear Accelerator Center, Stanford University, Stanford, California 94309

ABSTRACT

Background sources at the 1 TeV Next Linear Collider are discussed along with ideas on how to limit their effect on the detector. With modest shielding and an adequate solenoidal field, we find that detector backgrounds are minimal and that the experimental environment should be similar to that which one normally associates with e^+e^- colliders.

I. INTRODUCTION

Detector backgrounds at the NLC are expected to come from the following sources:

- Off-orbit particles in the beam tail interacting near the IP
- Muons produced when the beam tails are collimated
- Synchrotron radiation (SR) photons
- e^+e^- pairs produced in the beam-beam interaction
- Hadrons produced in the beam-beam interaction

Each of these sources has been discussed in the NLC Zeroth Order Design Report[1]. This paper will collect and summarize the ZDR results on backgrounds, augmenting them with new calculations motivated by discussions at Snowmass. Together with the companion papers in these proceedings that describe the current ideas for a compact detector and stable final focus doublet, it presents a coherent snap-shot of our understanding of the issues facing the experimenter.

II. DETECTOR ISSUES

In order to quantify tolerable levels of a given background, we use the experience of the SLD detector as a guide. Experience with SLD's vertex detector (VXD), based on 22 μm $\times$ 22 μm CCD pixels, has shown that hit density is the best figure of merit, as it controls track linking purity and efficiency. Integrating over its readout time of 19 bunch crossings, the SLD VXD2 averaged 0.4 hits/mm^2 in its innermost layer. As there were no difficulties in linking VXD hits to tracks extrapolated from the 80 layer drift chamber, 1 hit/mm^2 per unit of readout time has emerged as a conservative figure of merit for VXD backgrounds. In three to four layer self-tracking CCD vertex detectors, track extrapolation errors will be on the order of 10 μm and the detector will be robust against backgrounds 10 to 20 times worse.

Raw occupancy is the figure of merit for a gas tracking chamber comprised of a relatively small number of wires, each of which samples a large volume. The 5120 wire SLD chamber at $r = 20$ cm typically operates with 2-5% occupancy. Simulations [2] indicate that the hits arise from the interaction of between 10^3 and 10^4 photons, typically 50 keV to 1 MeV, produced from the secondary interactions of SR photons of average energy 2 MeV in the masking system. These convert with an efficiency of 2% and cause, on average, 1.5 wires to fire. We take 10^4 photons per train as the design goal for an NLC gas tracking chamber.

Muons produced in upstream collimators traverse the SLD barrel calorimeter at the rate of one or two per beam crossing. In bad running conditions there can be a factor of ten increase in the muon flux whence the schemes used to keep the muons from contributing to the trigger rate, and, to a lesser extent, the reconstructed energy, break down. The design goal of the NLC muon protection system is that 1% of the beam can be scraped off in the collimation section and produce, on average, one muon at the detector per bunch train.

This paper assumes that at the NLC the integration time for each detector spans the full train of 90 bunches. Depending on the technology actually used, this assumption may be overly pessimistic; nanosecond level timing and the ability to isolate background at the bunch level will certainly be a design goal for NLC generation detector components.

III. IR LAYOUT

Figure 1 shows the current masking and magnet layout in the interaction region (IR). The last quadrupole of the doublet (QFTA) is a SmCo permanent magnet that ends 2 m from the interaction point (IP). Its inner aperture radius is 4.5 mm and outer radius is 20 mm. A similar magnet with a larger aperture (6 mm radius) transports the outgoing disrupted beam, together with any SR and beamstrahlung photons. These two magnets are followed by a twin bore superconducting magnet to complete the doublet. Each will be surrounded by a superconducting coil, not shown nor yet modelled in EGS, which shields the detector's solenoidal field.

A “dead cone”, within which the vast majority of the low p_t e^+e^- pairs produced by the beam-beam interaction are confined, is defined by a conical tungsten mask, M1, which subtends the angular range from 100 to 150 mrad and 0.5 m$< z <$ 2 m. A cylindrical tungsten skirt, M2, 10 cm thick, begins at z=2.0 m and r=20 cm. Its purpose is to protect any exterior detector from photons produced when the pair electrons and positrons strike the front face of the quadrupoles or luminosity monitor. The beam pipe has a radius of 1.0 cm for the first 2.5 cm from the IP. This will accommodate the inner layer of a vertex detector with acceptance out to $\cos\theta = 0.9$. The beam pipe then flares to a radius of 2 cm, switching from Be to 1 mm thick stainless steel. Within the beam pipe is a thin rf shield septum which gradually makes the transition from the narrow apertures of the input and exit quadrupoles to the beam pipe radius.

*Work supported by the Department of Energy, contracts DE-AC03-76SF00515 and DE-FG02-92ER40715.

IV. ACCELERATOR BACKGROUNDS

Design calculations result in very low estimates for the amount of beam halo at the end of the linac; nevertheless, experience at the SLC indicates that as much as 1% of the beam may need to be collimated. This corresponds to $\sim 10^{10}$ particles per train of 90 bunches. A two-pass linear collimation system[3] occupies the first 2.4 km after the linac. It is designed to reduce the tail population to below 10^6 particles per train before the beam enters the phase space defining masks at the entrance to the final focus (FF). These masks limit the size of the beam transported through the FF to $8\sigma_x$ by $35\sigma_y$ which determines the maximum betatron orbit allowed in the FF and determines the amount of SR that can be generated. The limit of 10^6 is set by muon production and transport studies, described below, which estimate the muon background rate at the detector.

In the linac-IP layout of Figure 2 each final focus tunnel is placed at 10 mrad with respect to the collimation section. These "Big Bends", 2.2 km from the IPs, protect the detectors from muons produced by the collimators, provide a 20 mrad crossing angle between incoming and outgoing beams, and allow for two experimental halls with IPs separated by 40 m. As trains consisting of 90 bunches of 0.65 - 1.1×10^{10} particles separated by 1.4 ns will collide at 120 – 180 Hz, a crossing angle is required so that a given bunch interacts with only its partner, and not with any other bunch still travelling to the IP. Additionally, the bend allows for an independent and larger aperture extraction line, which makes it easier to cleanly capture disrupted beam particles and beamstrahlung-produced photons.

A. Collimator Section Sources

EGS studies of beam tail interactions at a collimator predict that 10% of the electrons that fall within the first 1 μm of its edge are rescattered into the beam with a characteristic scattering angle of 14 μrad; the rest are absorbed or lost. At the first set of collimators, the beam halo density per train is $\sim 10^{10}$/mm, resulting in 10^6 particles edge scattered back into the beam. As this is too close to the limit we allow for scraping in the FF, the number is reduced by a second, clean-up, set of collimators, optically separated from the first collimator set by 8 km (R_{12} in beam optics jargon). As the lattice spreads the halo over roughly 10 cm at this point ($\sim$ 14 μrad $\times$ 8 km), its density is only $\sim$ 10/μm, so that edge scattering should result in only one particle per train striking the final focus collimators.

In addition to edge scattering, beam-gas scattering is a potential source of particles that can hit downstream collimators. Assuming a conservative vacuum pressure of 10^{-8} Torr, $\sim 10^4$ particles are gas scattered onto both the clean-up collimators and the FF collimators. This number is negligible relative to edge scattered particles in the first case, but dominates at the FF. Nevertheless, there still exists a safety factor of 10^2 from the design goal of 1 muon per train entering the detector.

As the FF collimators themselves are optically separated from the clean-up collimator set by 10 km, there is *another* factor of 10^6 reduction in halo particles rescattering into the beam. Furthermore, TRANSPORT studies of these rescattered particles, show that fewer than one in 10^5 impact the final doublet. Beam tails at the last quadrupole from sources upstream of the FF collimators should thus be less than 10^{-7} per train and completely negligible.

B. Muon Production from Collimators

To study the background due to muons, the equivalent of more than 10^{14} electrons were made to interact in the collimation system and final focus. Muons, produced through the Bethe-Heitler process and positron annihilation, were transported through the tunnel with its 10 mrad bend to the IP, taking into account the lattice, scattering in the tunnel walls, magnet yokes and supports, and a system of tunnel-filling toroidal "spoiler" magnets

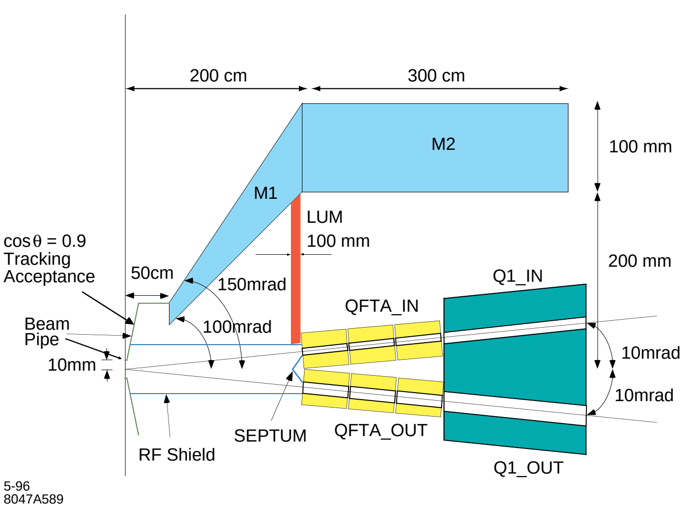

Figure 1: The interaction region masking and magnet layout.

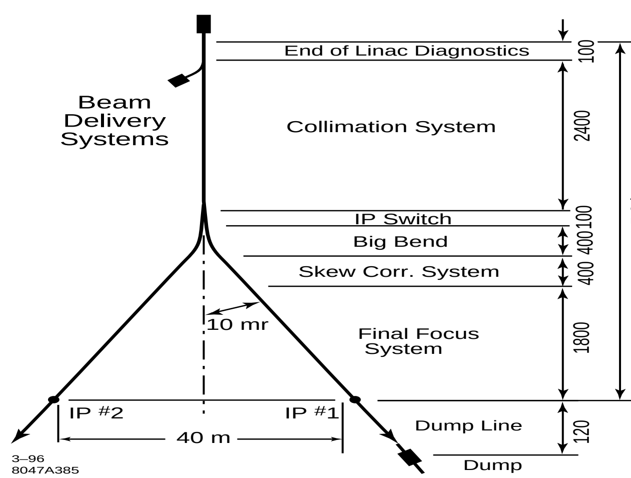

Figure 2: The general layout of the final foci and interaction regions. (Not to scale.)

strategically placed to intercept and further deflect muons.

Figure 3 shows the results of the calculation as a function of the source location. The ordinate is the number of electrons that must interact in order to produce one muon at a 8 m by 8 m detector at the IP. The positions of the collimators and muon spoiler toroids are indicated. In the uppermost of the two curves the calculation incorporated the tunnel-filling muon spoilers; the lower curve did not. One observes that the spoiler system adds three orders of magnitude of muon background protection in the collimation region and gives us a factor of 10^2 safety over the design goal (which corresponds to 10^{10} on this scale), and are thus required. In either case, we are most sensitive to beam particles lost in the FF after the big bend. Figure 3 shows that 3×10^7 particles lost on the first horizontal FF collimator will produce one muon that reaches the detector. Without the downstream spoiler magnets this is one muon per 10^6 particles on the collimator.

C. Final Focus Region Sources

We next consider background sources [4] generated between the FF collimators and the IP. All calculations assume 10^{12} particles per train and a vacuum pressure of 10^{-8} Torr. Beam-gas interactions result in 0.4 Coulomb scatters per train. Electrons which have lost between 6% and 25% of their energy due to bremstrahlung in the field of a residual gas nucleus may also impact the final doublet. Calculation indicates that 64 such electrons will be produced in the last km of beam transport. Additionally, the beam can also suffer inverse Compton scattering on thermally radiated photons. We calculate that 30 electrons will be scattered in the last km per train. Debris due to inelastic eN scattering is estimated to be completely negligible, less than $3{\times}10^{-4}$ per train. The scattering of two particles within the same bunch (Touschek effect) is likewise estimated to produce less than one scattered electon per train.

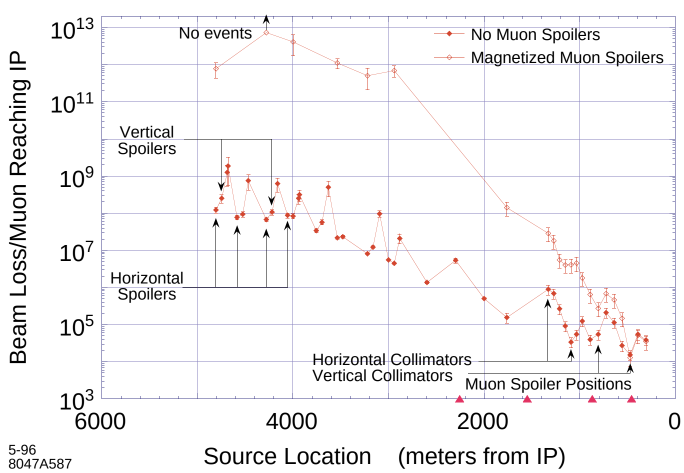

Figure 3: Amount of primary beam that must be lost at a given location in order to produce one muon that hits the detector. Data are presented for calculations with and without a system of tunnel-filling toroidal magnets.

While the FF collimator TRANSPORT study leads us to believe that a large fraction of these degraded electrons will not hit the final-doublet apertures, we have yet to fold production cross sections into a TRANSPORT calculation to make a quantitative estimate of the reduction. If these studies show regions of the FF with high transmission probability to the IP, they can be instrumented with better vacuum and more masking.

D. Effect of Particles Impacting Near the IP

While we have argued that their numbers are negligible, it is nevertheless of interest to estimate the detector backgrounds from near-full energy particles interacting near the IP. The maximum of the beam envelope in y in the final doublet [5] occurs $\sim 2/3$ of the way from the IP end of the quad nearest the IP, at about 3 m, and in x at the far end of the second quad, at $\sim$8 m. If off-energy particles are produced, these areas are the most likely place for them to strike the final doublet. Thus we have used EGS to simulate the interactions of 500 GeV particles incident at 1 μrad to the top and bottom of the inner 4.5 cm radius bore of the permanent magnet quad at a z of 3 m. A 500 keV (10 keV) cutoff energy is used for tracking secondary electrons (photons) from the interaction.

We find that particles exiting the sides of the quadrupole are soft and stop in the M2 mask. For each interacting beam particle, 9 e^+/e^- and 200 photons exit the front face with approximate azimuthal symmetry, and strike either the up-beam M1 mask or down-beam quadrupole. Figure 4 shows the average charged hit density from e^+, e^- and photons within an acceptance of $\cos\theta$=0.9 as a function of radius per interacting 500 GeV electron. The detector solenoidal field was taken to be 4 Tesla and the conversion efficiency for photons to charged hits as 1%. We see that at the smallest radii charged hits from this source are a factor of 10^3 below our target of 1 hit/mm^2/train, and a factor of 10^4 below the background density from SR or the beam-beam interaction. We should thus be insensitive to beam scraping at the $\sim$100 particle or less per train level predicted in section C.

E. Synchrotron Radiation

SR produced in the soft dipole bend just upstream of the final doublet and SR produced in the quadrupoles by particles at the edge of the phase space allowed by the collimation system can cause backgrounds in the detector. Most of the radiation escapes through the output quadrupole aperture; photons striking the inside of the incoming quadrupole aperture near its IP end are the biggest problem. The soft bend SR will be masked far from the IP. Figure 5 shows the energy distribution of SR from the beam tail as calculated for the 1 TeV c.m. lattice. As long as the QFTA aperture is large enough that radiation produced immediately upstream in Q1 can escape, the situation is not dramatic. If the QFTA aperture decreases below 4.3 mm radius, or the tail collimation is loosened beyond $7\sigma_x$ and $35\sigma_y$, the energy deposited in QFTA increases dramatically.

Figure 4 shows the results of the EGS simulation using the 4.5 mm aperture SR energy distribution of Figure 5 as input. The charged particle hit density due to directly produced e^+e^- pairs and due to photons are plotted as a function of radius for a 4 Tesla detector solenoidal field. The e^+e^- pairs are made when SR photons strike the lip of the quadrupole; very soft, they are guided by the detector's solenoidal field toward the IP. Their hit density is tolerable for $r \geq 2$ cm. The hit density due to converting photons is negligible in the region of the vertex detector. However, the photon density would correspond to having over 100,000 photons incident on a $|z| < 1$ m tracking chamber at $r = 30$ cm, which might preclude a conventional drift chamber. Tighter collimation would reduce these numbers, as would the 500 GeV c.m. lattice.

V. BEAM-BEAM BACKGROUNDS

A. Pairs

Roughly 10^5 e^+e^- pairs will be produced by the beam-beam interaction each bunch crossing, predominately through the Bethe-Heitler interaction of beamstrahlung photons and electrons or positrons. For the most part the pairs are produced with low intrinsic p_t; the same sign partner will tend to be focused by the opposing beam while the opposite sign partner will be deflected outside the beam envelope by the magnetic field of the bunch. The finite beam dimensions result in a hard kinematic edge in the $p_t - \theta$ distribution (Figure 6).

By introducing a strong solenoidal magnetic field all particles with $p_t < 30$ MeV are curled up within the 5 cm minimum radius of the conical mask of Figure 1. All particles with θ within the 100 mrad dead cone are contained regardless of their p_t. The number of particles falling outside these two cuts is relatively small and manageable.

We have simulated the beam-beam interaction at 1 TeV c.m. with the ABEL program. Figure 7 shows the hit density expected at $r = 2$ and 3 cm as a function of z for a solenoidal field of 4 Tesla. At $r = 2$ cm, as long as our VXD lies within $|z| \leq$ 17 cm, the hit density is manageable. Lowering the field would require that the innermost vertex layer be at a correspondingly larger radius.

B. Photons from Pairs

Pairs will interact with the beam pipe, inner vertex detector layers, rf shield septum, and front faces of the entrance and exit quads. As they interact, photons will be produced which will form a secondary background in the VXD and in any tracking chamber at larger radius.

To study this problem we have used a 1 TeV ABEL ray file as input to the EGS simulation of the IR of Figure 1. Figure 4 shows the charged hit density due to these backscattered pairs

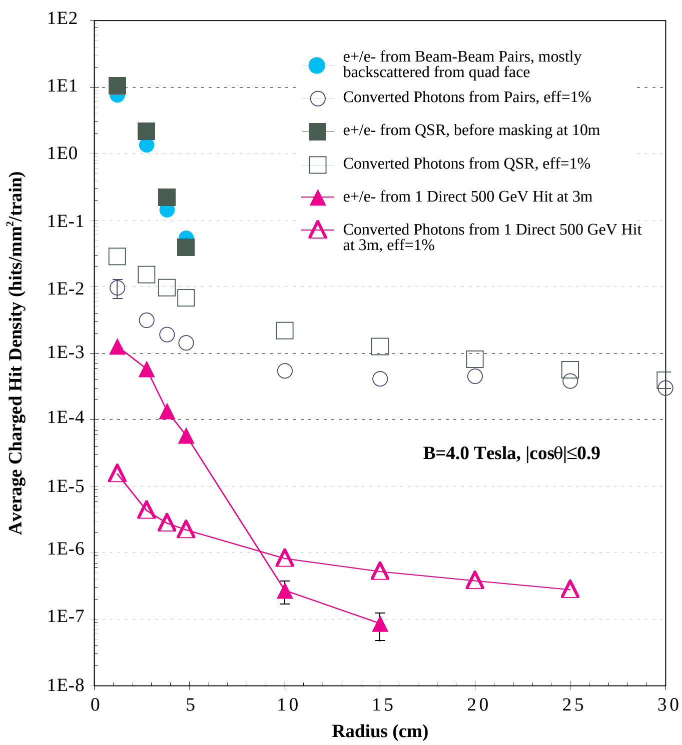

Figure 4: The charged hit density in the NLC detector as a function of radius due to electrons and photons produced by either beam scraping in the final doublet, beam-beam interaction produced e^+e^- pairs, or the interaction of SR produced photons. An angular acceptance of cosθ=0.9, a detector solenoidal field of 4 Tesla, and a photon coversion efficiency of 1% are assumed. All numbers are for two interacting trains of 10^{12} particles.

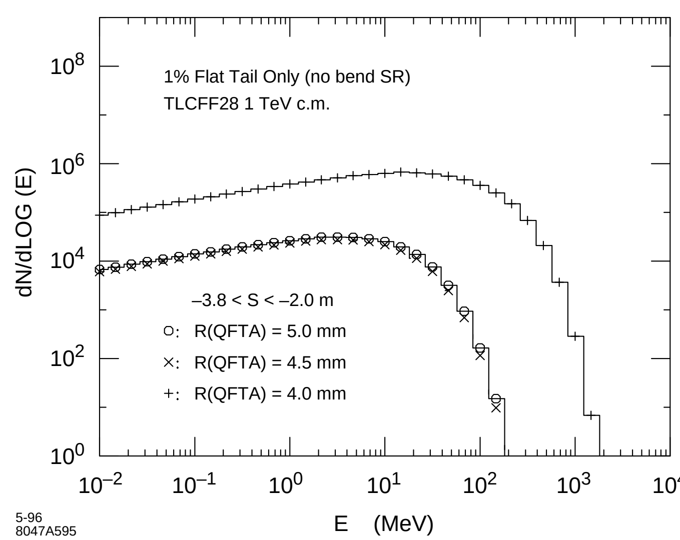

Figure 5: Energy distribution of SR photons, from particles in the assumed 1% flat tail of the beam, striking the inner aperture of QFTA, the innermost quad. When the aperture is small enough to intercept SR from the superconducting quadrupoles the incident flux is much larger, as shown for a 4.0 mm radius

and photons. The contribution from forward-going pairs is included, but, as explained in the previous section, is negligible with the 4 Tesla solenoidal field. The density is averaged over an angular acceptance of $\cos\theta = 0.90$. The photons are converted to charged hits assuming an efficiency of 1%. The hit densities are all well below 1/mm^2/train. However, as was the case for the SR source, the raw number of photons crossing the r=30 cm plane is rather large. While more innovative masking schemes may help, it does seem that low granularity tracking devices will be marginal in the NLC background environment.

C. Hadronic backgrounds from $\gamma\gamma$ Interactions

Hadronic background rates have been estimated [6] by folding the beamstrahlung photon energy distribution and hadron production cross sections using an equivalent photon approximation. Most of the hadronic events are minimum bias events with small transverse momentum and small center of mass energy. At 1 TeV c.m., the mean energy deposited within a calorimeter with $\cos\theta$=0.985 coverage is just 11 GeV. The average p_t of a $\gamma\gamma$ event is 0.9 Gev, much less than the physics scale of interest of $m_W/2$.

The rate for these events is estimated as 0.3 per bunch crossing for the most agressive collider designs. Each detector used in an analysis will require time resolution at the ns level so that we need not integrate the background over more than a few of the bunch crossings in a train of 90 bunches. A more quantitative understanding of the sensitivity of each analysis to these backgrounds requires a more detailed physics simulation than we have yet had the opportunity to carry out.

VI. CONCLUSION

There does not appear to be any fundamental problem in designing an IR and detector which maintains the machine luminosity, can handle the backgrounds, and do the physics.

We expect that additional masking along the beam line will further reduce the SR induced backgrounds. A M1 conical mask optimized for a 4 Tesla solenoid, covering the region 65-100 mrad, will allow more acceptance for physics analyses while improving its shielding effects from beam-beam pairs. The hit density near a radius of 1 cm is due to very soft particles; trapping them with low Z materials or channeling them with the quadrupole fringe field are possibilities under investigation. Moving the final quadrupoles closer to the IP, a possibility opened up by the concept of a compact high field detector, would ease optical and engineering tolerances; its effect on backgrounds needs to be investigated.

VII. REFERENCES

[1] The NLC Design Group, "Zeroth Order Design Report for the Next Linear Collider", *LBNL-5424, SLAC-474, UCRL-ID-124161, UC-414* (1996), hereafter, The NLC ZDR.

[2] S.S. Hertzbach, T. Markiewicz, and T. Maruyama, "Backgrounds at SLD 2000", SLD-TN-252, SLC-CN-411 (September, 1996).

[3] The NLC ZDR, pg.556-641.

[4] The NLC ZDR, pg.729-731.

[5] The NLC ZDR, pg.743-767.

[6] P. Chen, T. Barklow, and M. Peskin, "Hadron Production in $\gamma\gamma$ Collisions as a Background for e^+e^- Linear Colliders", SLAC-PUB-5773, (April, 1993).

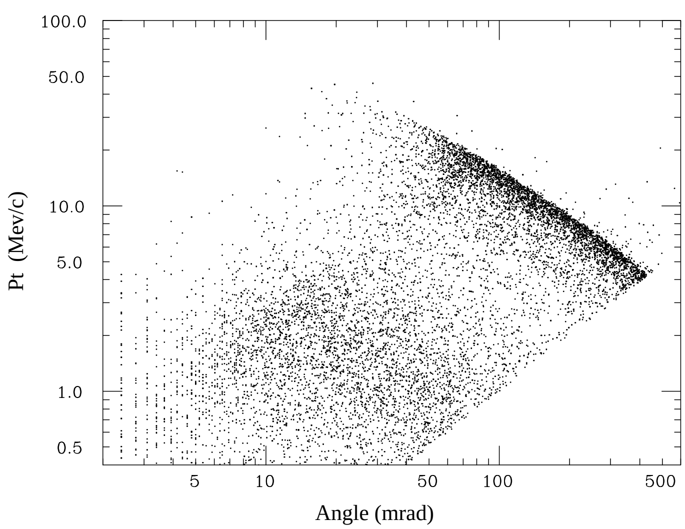

Figure 6: p_t vs.θ distribution for pairs.

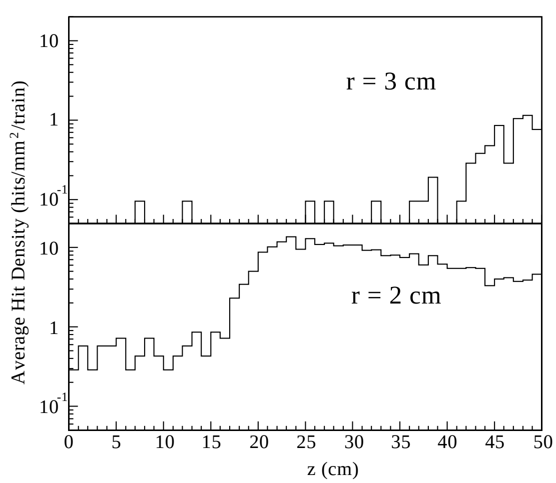

Figure 7: Electron pair hit density per mm^2 per train of 90 bunches, computed with the Monte Carlo program ABEL. As the pairs leave the IP in a 4 Tesla field, hits are scored at $r = 2$ cm and $r = 3$ cm.